Impurity effects on the Aharonov-Bohm optical signatures of neutral quantum-ring magnetoexcitons

L. G. G. V. Dias da Silva,[1,2] S. E. Ulloa,[2] and A. O. Govorov[2]
[1]*Departamento de Física, Universidade Federal de São Carlos, 13565-905 São Carlos SP, Brazil*
[2]*Department of Physics and Astronomy, Nanoscale and Quantum Phenomena Institute, Ohio University, Athens, Ohio 45701-2979, USA*
(Received 2 March 2004; revised manuscript received 21 June 2004; published 21 October 2004)

We study the role of impurity scattering on the photoluminescence (PL) emission of polarized magnetoexcitons. We consider systems where both the electron and hole are confined on a ring structure (quantum rings) as well as on a type-II quantum dot. Despite their neutral character, excitons exhibit strong modulation of energy and oscillator strength in the presence of magnetic fields. Scattering impurities enhance the PL intensity on otherwise "dark" magnetic field windows and nonzero PL emission appears for a wide magnetic field range even at zero temperature. For higher temperatures, impurity-induced anticrossings on the excitonic spectrum lead to unexpected peaks and valleys on the PL intensity as function of magnetic field. Such behavior is absent on ideal systems and can account for prominent features in recent experimental results.

DOI: 10.1103/PhysRevB.70.155318 PACS number(s): 71.35.Ji, 78.67.Hc

I. INTRODUCTION

A charged particle moving in a magnetic field acquires a phase proportional to the applied magnetic flux due to the quantum interference between different closed paths, giving rise to the long-studied Aharonov-Bohm effect (ABE).[1] This effect is specially important if the particle's configuration space has a ringlike topology, since the interference effects will create flux-dependent phase *differences* of characteristic size, which can be clearly identified in experiments.[2]

An interesting issue appears when one considers a system of bound charged particles, forming a *composite* neutral object. An example of such system is a ring-confined exciton, an optically active electron-hole bound state with experimentally accessible characteristics.

The optical manifestations of such excitonic Aharonov-Bohm effect in semiconductor quantum-ring structures has received great attention from both theoretical[3–15] and experimental[16–19] groups. Whereas one could imagine that no ABE should be expected for neutral particles, a small but nonvanishing ABE in neutral excitons confined in one-dimensional rings was theoretically proposed.[5–7] In such systems, the exciton's finite size allows for an internal polarization of the positive and negative charges in such a way that the magnetic flux phases acquired by the electron and hole do not cancel each other. The ABE amplitude in one-dimensional systems is shown to depend on the tunneling amplitude of either electron or hole to the "opposite side" of the ring and is exponentially suppressed when this tunneling amplitude decreases.[6,7] An enhancement of the ABE is also predicted when an in-plane electric field is applied.[8]

The ABE is further suppressed when a two-dimensional (2D) "ring stripe" is considered and both electron and hole are confined by a finite width potential.[9,10] However, if *different* confining potentials for the electron and hole are considered in the structure, a strong effect is expected on the photoluminescence intensity (PLI).[11–13] In this case, a net radial polarization of the exciton naturally exists and the ABE could be strong enough to be detected by photoluminescence (PL) experiments. The optical emission is predicted to oscillate as the ground-state angular momentum changes, generating a series of "dark" and "bright" PL emission regions as function of the magnetic flux. The same underlying principle applies in the study of the PL response in semiconductor quantum dots with type-II band alignment.[13,14,20]

The ABE on charged[17] and neutral excitons[18] has been reported in recent beautiful experiments and found to be in general agreement with expectations. Although the above mentioned "dark windows" have not been experimentally reported for the case of neutral excitons confined in self-assembled quantum rings,[19] experimental evidence of the ABE was found in photoluminescence experiments using type-II quantum dots samples.[18] Some of the findings, however, remain not completely understood and interesting questions remain open. For example, the experimental field-dependent PL intensity does not fully agree with the expected result in quantum rings.[18,21] Moreover, as the PL signal is collected from an ensemble of dots/rings over a large area, the role of impurities cannot be neglected.

In this paper, we discuss the effect of impurity scattering on the optical properties of quantum rings and study the influence of perturbative defects in the optical Aharonov-Bohm effect in these systems. Previous treatments of disorder effects in magnetoexcitons in quantum-rings have focused attention on the underlying dynamics of the electron-hole dipole moment.[24] We choose a different approach, concentrating on the effects of symmetry-breaking in the optical emission intensity.

Our main results can be summarized as follows: even though impurity scattering leads to mixing of angular momentum states, signatures of the Aharonov-Bohm effect on a neutral exciton remain for significant impurity strengths. We further find that finite temperatures not only produce the monotonic smoothing of spectral features, but also induce

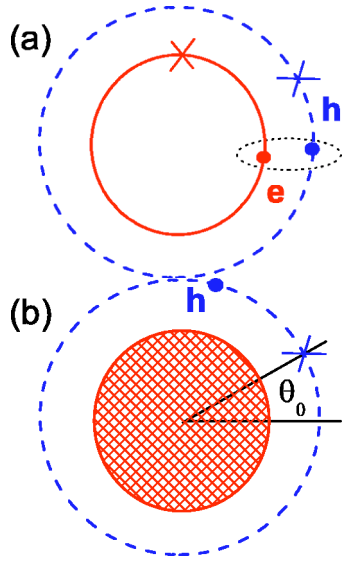

FIG. 1. Schematic representation of a polarized neutral exciton in a quantum ring (top) and in a type-II quantum dot (bottom)

additional characteristics in the PLI that can be attributed to impurity effects. In fact, this suggests the use of disorder-induced ABE features as a tool to probe into the impurity potentials and extract information on the confining strength and localization length of the hole and electron wave functions. Additionally, we will discuss how our results can account for recent experimental data on the PLI of type-II QDs.[18]

The paper is organized as follows: a general description of the studied systems and the theoretical models is given in Sec. II. Results for the spectrum are given in Secs. II A and II B. The PL emission, the core result of the paper, is presented in Sec. III, while our overall conclusions are given in Sec. IV.

II. THEORETICAL MODEL

The systems to be modeled display a polarized neutral exciton confined on a 2D ringlike geometry and subjected to a perpendicular magnetic field. The confining radii can be different for electrons and holes due to sample strain and different carrier masses, giving rise to a net radial polarization of the electron-hole pair. A natural assumption is that the radial confining width w is small ($R/w \gg 1$) for at least one of the carriers.

If both electrons and holes are strongly confined in the radial direction, the corresponding dynamics is essentially one dimensional and can be described by two concentric rings as on the left panel in Fig. 1(a) (henceforth referred to as *polarized quantum ring*).

On the other hand, if only the outer carrier is strongly confined radially, then the inner carrier's wave function has a more extended character and the system will have a type-II quantum dot characteristic distribution of carriers [Fig. 1(b)]. In this situation, the confining potential profile is such that one of the carriers is confined inside the dot while the other is kept spatially separated on the outside. For disklike quantum dots, the outside carrier is kept on a ring trajectory due to the Coulomb attraction between the carriers. In both cases, the polarized nature of the neutral exciton gives rise to oscillations on the ground state energy as the magnetic flux through the ring changes, due to the accumulation of a net Aharonov-Bohm phase on the electron-hole pair wave function.[11–13]

The parameters used in the remaining of the paper model the experimental system described in the work of Ribeiro and collaborators.[18] Namely, we set the effective masses $m_e^*=0.073m_e$, $m_h^*=0.255m_e$, and ring radii $R_e=16$ nm and $R_h=19$ nm in our calculations. Those values for $R_{e(h)}$ come from direct imaging of the structures as well as from fitting the observed spectral features. We also consider the experimental value for the size dispersion in the dots: $\Delta R \approx 0.8$ nm, an important element in comparison with experiments. Notice that we consider only the heavy hole exciton, as strong vertical quantization in the dots (or rings) break the light-heavy hole degeneracy found in bulk materials.

In addition, we consider the effect of scattering impurities on the ring trajectories. For such structural parameters, typical single-particle confinement energy scales are 0.1–0.5 meV. It is clear from the outset that if charged impurities with strong trapping potentials of order $U \sim 5$ meV were present, the corresponding wave function localization would be so large that the Aharonov-Bohm oscillations could not survive. We then consider perturbative impurity effects, with weak potential strengths that may arise from local strain effects due to lattice mismatches, distant charge centers and other lattice defects near the InP/InAs interfaces.[21] For concreteness, we use the impurity potential strength as $U_h^{\mathrm{imp}}=+0.015$ meV, and $U_e^{\mathrm{imp}}=-0.023$ meV for holes and electrons, respectively, unless otherwise stated.

One should notice that even though our energy and length scales are set for comparison with the experiment, the validity of our results is not restricted to those parameters. In fact, as we will see, our predictions hold as long as $U^{\mathrm{imp}} \ll \hbar^2/2m^*R^2$.

A. Polarized quantum ring

We first consider the case where the confining width for *both* carriers is small compared to the ring radius and include single and multiple δ-scattering impurities along the confining region. The impurities are located on fixed angular positions θ_i^0 (which can be different for electrons and holes). The Hamiltonian for the polarized quantum ring reads

$$H = \frac{\left(\mathbf{p}_e - \frac{e}{c}\mathbf{A}(\mathbf{r}_e)\right)^2}{2m_e^*} + \frac{\left(\mathbf{p}_h + \frac{e}{c}\mathbf{A}(\mathbf{r}_h)\right)^2}{2m_h^*} + V_{\mathrm{ring}} + \sum_{ij} U_e^{\mathrm{imp}}\delta(\theta_e - \theta_i^0) + U_h^{\mathrm{imp}}\delta(\theta_h - \theta_j^0) + V_{eh}(\mathbf{r}_e, \mathbf{r}_h), \tag{1}$$

where $m_{e(h)}^*$ are the electron (hole) effective masses, **A** is the

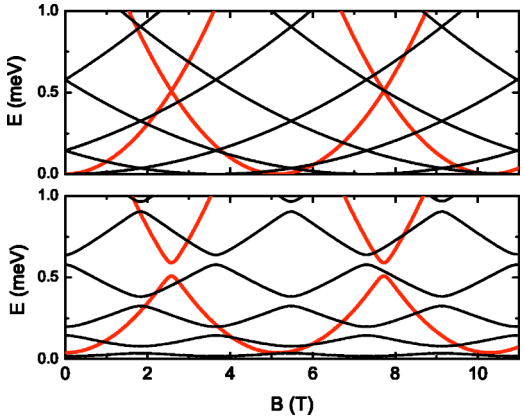

FIG. 2. (Color online) Electron (red thick line) and hole (black thin line) energy levels as function of magnetic field for the unperturbed (top) and impurity-distorted (bottom) cases.

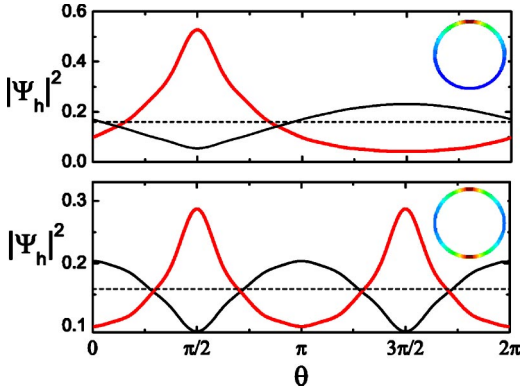

FIG. 3. (Color online) Hole probability ground-state distribution for attractive (red line and insets) and repulsive (black line) impurities at $\theta_0=\pi/2$ (top panel) and two impurities at $\theta_0=\pi/2$ and $\theta_0=3\pi/2$ (bottom panel). Dashed line shows the uniform $(2\pi)^{-1}$ probability density for the unperturbed case.

vector potential, and $U^{\rm imp}_{e(h)}$ are the electron (hole) impurity strengths. The last term is the Coulomb electron-hole interaction.

Following the preceding discussion, the effective Bohr radius for our reference system will be of order $a^*_B\sim 10$ nm. Therefore, even though $R/a^*_B\sim 2$, we have $w/a^*_B\ll 1$ if the radial confining width w is small ($R\gg w$). An estimate for the confining and Coulomb energies gives $\hbar^2/2m^*w^2\sim 60$ meV and $e^2/\varepsilon_r a^*_B\sim 10$ meV, respectively, for $w\sim 3$ nm and $a^*_B\sim 10$ nm. Since our main interest resides on the impurity effects in strongly confined noncharged excitons ($w/a^*_B\ll 1$), the attractive interaction V_{eh} has a perturbative effect in the level structure and its main effect is to provide weak correlation effects and a constant binding energy shift $E^B_{\rm exct}$, which we can safely ignore.[22] We should mention that, for strong interactions, an interesting coherent drag effect may reveal itself in the flux dependence of the photoluminescence, akin to the case of electronic systems.[23]

The unperturbed ($U^{\rm imp}_{e(h)}=0$) Hamiltonian is separable and can be solved analytically. The angular energies and eigenfunctions are given by

$$E^{(0)}_i(l_{e(h)})=\frac{\hbar^2}{2m_{e(h)}R^2_{e(h)}}\left(l_{e(h)}\mp\frac{\Phi_{e(h)}}{\Phi_0}\right)^2, \tag{2}$$

$$\varphi^{e(h)}_i(\theta)=\frac{1}{\sqrt{2\pi}}e^{il_{e(h)}\theta}\equiv\langle\mathbf{r}|l_{e(h)}\rangle, \tag{3}$$

where $R_{e(h)}$ and $l_{e(h)}$ are the electron (hole) confining radius and angular momentum value, respectively, $\Phi_{e(h)}=\pi R^2_{e(h)}B$ are the individual fluxes and $\Phi_0=h/e$ is the unit quantum flux. The energy levels of electron and hole on the ring are shown on the top panel of Fig. 2.

In this model, the excitonic states are given by a superposition of electron and hole states $|\Psi_{\rm exct}\rangle=|l_e\rangle\otimes|l_h\rangle$. These states have well-defined angular momentum values given by $L=l_h+l_e$, and energies given by $E^{\rm exct}=E^{(0)}_e+E^{(0)}_h$. The ground state angular momentum changes whenever either Φ_e/Φ_0 or Φ_h/Φ_0 is a half-integer. In a unperturbed system, momentum changes of the ground state result in sharp dark↔bright transitions in the PL of the QR.[11]

The impurities are included by numerical diagonalization of Hamiltonian (1) in this $\{|\Psi_{\rm exct}\rangle\}$ basis. The single-particle matrix elements $\langle l'|U^{\rm imp}|l\rangle$ can be calculated analytically, giving

$$\langle l'|U^{\rm imp}|l\rangle=\left(\frac{U^{\rm imp}}{2\pi}\right)\sum_j e^{i\Delta l\theta^0_j}, \tag{4}$$

where $\Delta l=l-l'$, and θ_0 is the angular position of the impurity, as shown in Fig. 1(b). From Eq. (4), one can readily see that the impurity potential breaks the rotational symmetry of the system since it couples all $\{|l\rangle\}$ states. Thus, the excitonic states will no longer have definite angular momentum but rather be a linear combination of the form

$$|\Psi^{\rm exct}_k\rangle=\sum_{l_h}C^h_{l_h,k}C^e_{l_e,k}|\varphi^h_{l_h}\rangle\otimes|\varphi^e_{l_e}\rangle. \tag{5}$$

The effect of such symmetry breaking on the energy levels is seen in Fig. 2 in the case of a single impurity. All the level crossings at magnetic field values where $\Phi_{e(h)}/\Phi_0=n/2$, present in the unperturbed system (top panel), become *anticrossings* with width proportional to $U^{\rm imp}_{e(h)}$, as shown in the bottom panel. It is worth mentioning that the spectrum remains unchanged under angular displacements of the single impurity, since $\theta^0\to\theta^0+\Delta\theta$ only gives a phase to the matrix elements (4).

As a consequence of impurity scattering and of the attractive Coulomb interaction, both the hole and electron wave functions tend to be localized around θ^0_i. This effect is shown in Fig. 3 for the hole probability density $|\psi_h(\theta)|^2$ for one impurity, as well as for the case of two impurities separated by a distance $\Delta\theta$ at $B=0$. In the latter case, the wave function is pinned at θ_0 and $\theta_0+\Delta\theta$ when $U^{\rm imp}<0$ and is repelled from these angles for $U^{\rm imp}>0$. We find this pinning to be only weakly dependent on magnetic field.

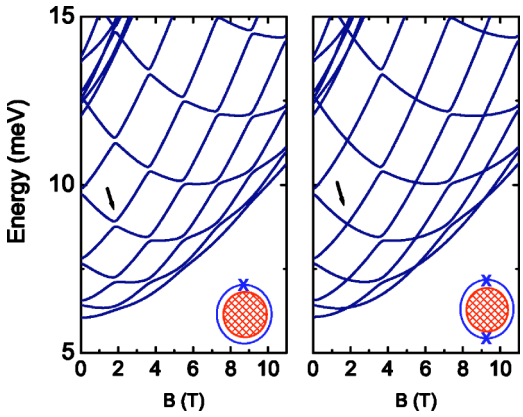

FIG. 4. (Color online) Excitonic energy levels as function of magnetic field on a type-II quantum dot for one impurity (left-hand side) and two symmetrical impurities (right-hand side). Some level crossings are restored in the symmetrical configuration, as indicated by arrows.

B. Type-II quantum dots

The Hamiltonian for the type-II ring-confinement model reads

$$H = H_{\mathrm{Dot}} + \frac{1}{2m_h^*}\left(\mathbf{p}_h + \frac{e}{c}\mathbf{A}(\mathbf{r}_h)\right)^2 + V_{\mathrm{ring}} + \sum_i U_h^{\mathrm{imp}}\delta(\theta_h - \theta_i^0) + V_{e-h}(\mathbf{r}_e, \mathbf{r}_h), \tag{6}$$

where H_{Dot} describes the electron confined in a parabolic dot with a characteristic frequency ω_0 and under the influence of a magnetic field. In the absence of spin-orbit interactions, the electron energies are given by the Fock-Darwin levels,

$$E^e_{nl\sigma} = (2N + |l| + 1)\hbar\Omega + \frac{l}{2}\hbar\omega_c + g\mu_B\frac{B\sigma}{2}, \tag{7}$$

where N is a positive integer, l is the angular momentum, ω_c is the cyclotron frequency and $\Omega = \sqrt{\omega_0^2 + \omega_c^2/4}$ is the effective electron frequency. The Zeeman splitting term does not alter our results qualitatively and is disregarded in the following calculations.

We focus on impurity effects on the hole outside the QD. Notice that (i) the effects of impurity scattering are stronger on the 1D hole confinement as compared to the electronic 2D confinement and (ii) the ABE reflects the phase acquired by the hole wave function and would not be significatively affected by scattering processes inside the quantum dot.

The excitonic energy levels obtained from (6) in the strong confinement regime are shown in Fig. 4, for the cases with one and two impurities. The low-lying states correspond to the combination of the first electronic states ($l_e = 0$) with low-lying hole states. As in the polarized QR case, the impurity potential induces anticrossings on the whole spectrum.

When two impurities in a symmetrical configuration are present, some of the crossings are recovered as the π-rotational symmetry is recovered in the system. In this case, the coupling given by Eq. (4) vanishes whenever Δl_h is an odd number. In terms of symmetry, such arrangement is equivalent to having an *elongated* ring instead of a circular one. As a consequence, the anticrossings at $\Phi_h/\Phi_0 = n/2$ with odd n disappear while the ones at even n remain, as seen in the right-hand panel of Fig. 4.

III. PL EMISSION INTENSITY

Once the spectral characteristics of the system are obtained, the photoluminescence emission intensity can be calculated. We consider optical interband transitions near the Γ point of the solid. Since the photon angular momentum is taken up by the conduction-valence band transition matrix element, the emission intensity is proportional to the probability of finding the exciton on the $L=0$ state and also to the overlap between the electron and hole wave functions. The optical emission occurs then only if $l_e = -l_h$. This represents the *selection rules* on the electron emission.[11–13] If the exciton is on state $|\Psi_i^{\mathrm{exct}}\rangle$, the emission intensity I_i is then given by

$$I_i \propto |A_i|^2 P_i^{L=0}, \tag{8}$$

with

$$P_i^{L=0} = \left| \int \Psi_i^{L=0}(\mathbf{r}, \mathbf{r}) d\mathbf{r} \right|^2, \tag{9}$$

and where $\Psi_i^{L=0}$ is the projection of the excitonic state in the $L=0$ state, given by

$$\Psi_i^{L=0}(\theta, \theta) = \sum_{l_h} C^h_{l_h,i} C^e_{l_e,i} \varphi^h_{l_h}(\theta) \varphi^e_{(l_e=-l_h)}(\theta) \Rightarrow \int \Psi_i^{L=0}(\theta, \theta) d\theta = \sum_{l_h} C^h_{l_h,i} C^e_{l_e(=-l_h),j}. \tag{10}$$

In Eq. (8), $|A_i|^2$ is the electron-hole overlap radial integral. As discussed in Sec. II A, the wave functions tend to be localized near the impurities due to the electrostatic impurity trapping and to the Coulomb interaction between the carriers. Such localization modifies the overlap integral $|A|^2$, and therefore the emission intensity. However, once the wave functions are localized on the angular variable, the radial overlap has only a weak dependence with field, as long as the radial confinement is strong. Since we are interested on how the intensity changes with magnetic field, we take $|A|^2$ constant for simplicity since it does not alter our field-dependent results qualitatively.

The total emission intensity at a temperature T will be given by the thermal population average over the emission from different states,

$$I_{PL} = \frac{\sum I_i e^{-\beta E_i^{\mathrm{exct}}}}{\sum e^{-\beta E_i^{\mathrm{exct}}}}, \tag{11}$$

where $\beta = (k_B T)^{-1}$ and E_i^{exct} is the energy of the ith excitonic state.

When impurities are considered, the total angular momentum L is no longer a good quantum number since the

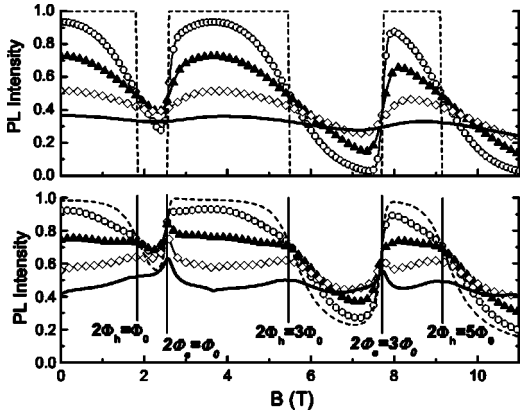

FIG. 5. Photoluminescence intensity as function of magnetic field for unperturbed (top) and single impurity-distorted (bottom) cases at different temperatures: $T=0$ K (dashed line), $T=0.5$ K (circles), $T=1$ K (triangles), $T=2$ K (diamonds), and $T=4$ K (thick line). The vertical lines in the bottom panel are guides to the eye, displaying the magnetic field values for $\Phi_{h(e)}/\Phi_0=n/2$.

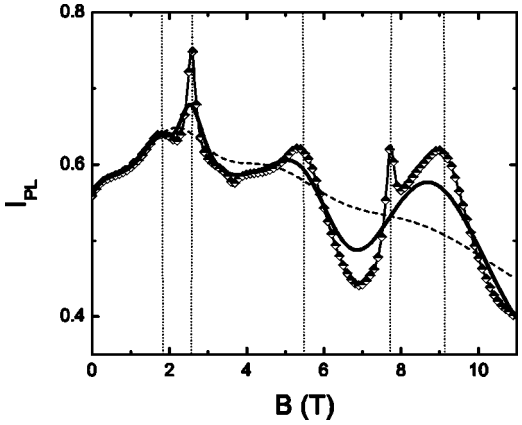

FIG. 6. PL intensity as function of magnetic field for the impurity-distorted case for $T=2$ K. Diamonds denote the intensity for fixed $R_h=19$ nm and $R_e=16$ nm. Thick and dashed lines denote size-averaged intensities, with Gaussian dispersions $\Delta R=0.8$ nm and $\Delta R=2$ nm, respectively.

impurity scattering mixes the angular momentum states. Therefore, a finite emission intensity is expected for all magnetic field values, unlike the situation in the unperturbed system which exhibits sharp transitions to bright exciton states.

A. Quantum rings

When both the hole and the electron are confined on a ring structure, the overall picture differs from the type-II quantum dot case. For the unperturbed case and at zero temperature, the PLI displays sudden drops whenever the excitonic ground state angular momentum goes to $L\neq 0$ states, i.e., whenever $\Phi_{h(e)}/\Phi_0$ is a half-integer. This leads to a series of dark and bright exciton windows in magnetic field,[11] shown as a dashed line in the top panel in Fig. 5. For higher temperatures, the thermal occupation of higher excitonic states smoothes out the transitions.

Impurity scattering changes this picture qualitatively in this spectrum as well, and introduces new field-dependent features on the PL intensity. As one impurity is added to the system, the PLI is nonzero for all magnetic field values *even at zero-temperature*, with a mean-value larger than in the unperturbed case (dashed line in the bottom panel in Fig. 5). This is a direct consequence of angular momentum mixing since the ground state will always have an $|L=0\rangle$ component for all values of magnetic field.

For higher temperatures, a pronounced peak appears at $\Phi_e/\Phi_0=1/2$ ($B\approx 2.6$ T) due to a ground state anticrossing (see Fig. 2). Additional peaks and valleys can be seen for higher temperatures due to anticrossings in the excited states, in a similar fashion as to the type-II quantum dot case. However, an important difference is that peaks are seen for magnetic field values where *either* Φ_e/Φ_0 *or* Φ_h/Φ_0 is a half-integer. The features for electrons are sharper due to their smaller mass and steeper level dispersions.

These findings could contribute to the understanding of recent experimental results on photoluminescence of neutral excitons in InP/GaAs type-II quantum dots.[18,21] Modulations on the PLI are found at magnetic values which are delayed with respect to $\Phi_h/\Phi_0=n/2$. These magnetic field values would correspond well to changes in Φ_e/Φ_0 had the electron been on a ring structure with a radius equal to the estimated QD radius R_{Dot}. Our results show that the presence of impurities and the effective QR structure would give rise to fluctuations at these magnetic field values.

A similar modulation of the PL intensity could be obtained if the electron wave function in the dot is more localized near the dot's edges than on its center. Such localization may occur if the bottom of the conduction band is not uniform but deeper at the edges, an effect which could be attributed to built-in strain in the sample.[25,26] Along with the Coulomb attraction between the electron and the hole, this would give rise to an effective ringlike configuration for the electronic wave function, similar to the one treated in this section.

Such features on the PL intensity could also be used to have an experimental access into the characteristics of the disorder potential. The size of the energy gaps in the spectrum (Fig. 2) are directly related to the impurity strength U^{imp}. The results presented in this section use $U_e^{\mathrm{imp}}\approx 0.02$ meV and $U_h^{\mathrm{imp}}\approx 0.04$ meV, which yields gaps of about $\Delta E_e\approx 0.08$ meV for electrons and $\Delta E_h\approx 0.06$ meV for holes. Although fine tuning of those parameters is clearly possible, it is interesting that such relatively small values lead to strong modifications of the exciton spectra.

There is an additional important consideration. The results so far consider a single polarized QR and a pertinent inquiry is what would be the effect of the size distribution of the structures used in experiments. We can consider these effects assuming a ring ensemble with Gaussian distributed radii (Fig. 6). As a general trend, a broad size distribution tends to blur the impurity effects, specially at higher magnetic fields. However, if the size distribution is as found in experiments ($\Delta R/R_0\approx 4\%$), these impurity-related effects are still seen for magnetic field values of order $\Phi/\Phi_0\sim 1$ ($B\approx 4$ T). We should especially mention that peaks in the PLI at certain

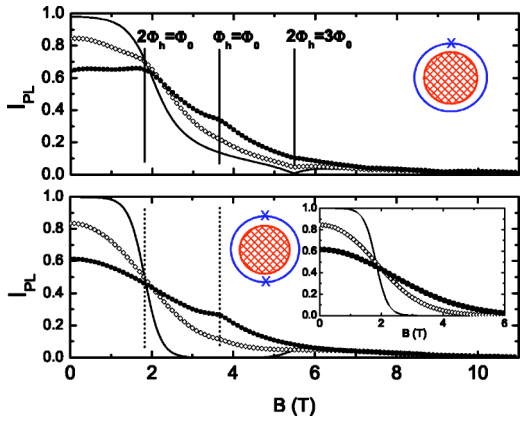

FIG. 7. Photoluminescence intensity as function of magnetic field for a electron-hole pair on a type-II QD with one (top) and two symmetric impurities (bottom). Curves for $T=0.5$ K (solid), $T=2$ K (diamonds), $T=4$ K (filled circles) are shown. Vertical lines are guides to the eye, representing $\Phi_h/\Phi_0=n/2$. Inset, intensity curves for the no-impurity case.

flux values are quite robust to ensemble average, even as the dark/bright exciton transitions are made smoother.

We summarize this discussion by saying that the systematics of this behavior, robustness to ensemble average and temperature effects, and even qualitative agreement with experiment, definitively point out for an effective QR geometry of the system.

B. Type II quantum dots

The plots in Fig. 7 show the photoluminescence intensity as function of the magnetic field for the type-II quantum dot magnetoexciton. For the unperturbed case (shown in the inset), a clear drop is seen after $\Phi_h/\Phi_0=1/2$ ($B\approx 1.8$ T for $R_h=19$ nm), when the hole ground-state angular momentum l_h changes from 0 to 1. This is a consequence of the emission selection rules. For low temperatures, the emission comes mainly from the ground state and therefore the drop is more abrupt. For higher temperatures, the $L=0$ excited states contribute to the emission and the drop in intensity is smoother.

The presence of impurities changes this behavior qualitatively. The cases of both single and double symmetric defects are shown in the top and bottom panels of Fig. 7, respectively. The excitonic states are linear combinations of states with different L, so that a nonzero $L=0$ component is present on the ground state even above $\Phi_h/\Phi_0=1/2$. Therefore, the low temperature drop in the intensity is much less abrupt than in the unperturbed case, as expected.

It is interesting, moreover, that at higher temperatures new PLI features arise when $\Phi_h/\Phi_0=n/2$ ($n=1,2,3,\ldots$). In the single impurity case, anticrossings occur at $n=1,3,5,\ldots$ (involving the ground state and first excited state), and also at $n=2,4,\ldots$ (between the first excited state and the second excited state) as shown in the left-hand panel of Fig. 4. At these anticrossings, the $|L=0\rangle$ components of the crossing states switch. If one of the crossing states had large $|L=0\rangle$ component (i.e., "$L=0$ character") before the crossing, it will likely have a smaller component after the crossing. These changes in character for the first excited states give rise to small peaks or dips on the overall PLI at higher temperatures. At $n=1$, for instance, as the ground state changes from "$L=0$ character" to "$L=1$ character," the opposite happens to the first excited state. This "$L=1\rightarrow L=0$" character transition on the excited state will give a positive second-order contribution to the intensity. Most importantly, at $n=2$, even though there is no ground state crossing, the second excited state has a "$L=2\rightarrow L=0$" change in character, which also manifests itself as a peak on the PLI for $T>2$ K (see spectrum in bottom panel of Fig. 4). On the other hand, this state's character changes "$L=0\rightarrow L=3$" at $n=3$, which in turn gives a negative contribution, seen as a sharp dip on the PLI at $\Phi_h/\Phi_0=3/2$. These variations in PLI versus magnetic field at well-defined multiples of the AB flux provide then unique features that one can relate to the role of impurity/defect potentials affecting the exciton.

For the special case of two symmetrical impurities in the ring, an additional symmetry is introduced in the system and the coupling between adjacent angular momentum states vanishes. The effect on the intensity is that a plateau near zero intensity is seen for low temperatures between $B\approx 2$ T ($\Phi_h/\Phi_0\approx 1/2; l=0\rightarrow 1$ transition) and $B\approx 5$ T ($\Phi_h/\Phi_0\approx 3/2; l=1\rightarrow 2$ transition), before the PLI grows again for $B\gtrsim 5.5$ T.

IV. CONCLUDING REMARKS

We have considered the effects of disorder on the Aharonov-Bohm effect in the optical emission of type-II quantum dots and quantum rings. As a general trend, the scattering potential breaks the rotational symmetry, thus coupling the angular momentum states. The effect of weak impurities does not preclude the Aharonov-Bohm oscillations in the optical spectrum, but rather induces additional features on the photoluminescence intensity at certain magnetic field values. Experimental systems have routinely high mobilities, yet some disorder is present and these PLI features could provide additional information on the structure of the impurity potential. They can also be used to probe the symmetries of the quantum rings, allowing, for example, one to discern between a circular structure and an elongated one.

Furthermore, our results could give insights on unexplained experimental results seen on the Aharonov-Bohm effect in neutral InP type-II quantum dot excitons.[18] Our analysis suggests that the unexpected magnetic field behavior of the intensity seen in the experiment could be explained if disorder and specific confinement of electrons and holes are taken into account.

ACKNOWLEDGMENTS

The authors would like to thank Evaldo Ribeiro, Gilberto Medeiros-Ribeiro, and Mikhail Raikh for valuable conversations and suggestions. This work was supported by FAPESP (Grants Nos. 01/14276-0 and 03/03987-9), the US DOE (Grant No. DE-FG02-91ER45334), and the Volkswagen Foundation.

[1] Y. Aharonov and D. Bohm, Phys. Rev. **115**, 485 (1959).
[2] R.G. Chambers, Phys. Rev. Lett. **5**, 3 (1960); A. Tonomura *et al.*, *ibid.* **48**, 1443 (1982); R.A. Webb *et al.*, Phys. Rev. Lett. **54**, 2696 (1985); For a review, see M. Peshkin and A. Tonomura, *The Aharonov-Bohm Effect*, Lecture Notes in Physics 340 (Springer-Verlag, Berlin, 1989).
[3] P. Pereyra and S.E. Ulloa, Phys. Rev. B **61**, 2128 (2000).
[4] A.O. Govorov and A.V. Chaplik, JETP Lett. **66**, 454 (1997).
[5] A.V. Chaplik, JETP Lett. **62**, 900 (1995).
[6] R.A. Römer and M.E. Raikh, Phys. Rev. B **62**, 7045 (2000).
[7] R.A. Römer and M.E. Raikh, Phys. Status Solidi B **221**, 535 (2000).
[8] A.V. Maslov and D.S. Citrin, Phys. Rev. B **67** 121304(R) (2003).
[9] J. Song and S.E. Ulloa, Phys. Rev. B **63**, 125302 (2001).
[10] H. Hu, J.-L. Zhu, D.-J. Li, and J.-J Xiong, Phys. Rev. B **63**, 195307 (2001).
[11] A.O. Govorov, S.E. Ulloa, K. Karrai, and R.J. Warburton, Phys. Rev. B **66**, 081309(R) (2002)
[12] S.E. Ulloa, A.O. Govorov, A.B. Kalameitsev, R.J. Warburton, and K. Karrai, Physica E (Amsterdam) **12**, 790 (2002).
[13] A.O. Govorov, A.B. Kalameitsev, R.J. Warburton, K. Karrai, and S.E. Ulloa, Physica E (Amsterdam) **13**, 297 (2002).
[14] A.B. Kalameitsev, V.M. Kovalev, and A.O. Govorov, JETP Lett. **68**, 669 (1998).
[15] J.I. Climente, J. Planelles, and W. Jaskolski, Phys. Rev. B **68** 075307 (2003).
[16] A. Lorke, R.J. Luyken, A.O. Govorov, J.P. Kotthaus, J.M. Garcia, and P.M. Petroff, Phys. Rev. Lett. **84**, 2223 (2000).
[17] M. Bayer, M. Korkusinski, P. Hawrylak, T. Gutbrod, M. Michel, and A. Forchel, Phys. Rev. Lett. **90**, 186801 (2003).
[18] E. Ribeiro, A.O. Govorov, W. Carvalho, and G. Medeiros-Ribeiro, Phys. Rev. Lett. **92**, 126402 (2004) (for intensity fluctuations, see cond-mat/0304092v1).
[19] D. Haft, C. Shulhauser, A.O. Govorov, R.J. Warburton, K. Karrai, J.M. Garcia, W. Schoenfeld, and P.M. Petroff, Physica E (Amsterdam) **13**, 165 (2002).
[20] K.L. Janssens, B. Partoens, and F.M. Peeters, Phys. Rev. B **66** 075314 (2002).
[21] E. Ribeiro and G. Medeiros-Ribeiro (private communication).
[22] J. Sierra-Ortega, S.E. Ulloa, and A.O. Govorov (unpublished).
[23] T.V. Shahbazyan and S.E. Ulloa, Phys. Rev. B **55** 13 702 (1997).
[24] K. Maschke, T. Meier, P. Thomas, and S.W. Koch, Eur. Phys. J. B **19**, 599 (2001).
[25] Z. Xu and P.M. Petroff, J. Appl. Phys. **69**, 6564 (1991).
[26] M. Tadic, F.M. Peeters, K.L. Janssens, M. Korkusinski, and P. Hawrylak, J. Appl. Phys. **92**, 5819 (2002).